

See discussions, stats, and author profiles for this publication at: <https://www.researchgate.net/publication/23455448>

# Inorganic Metal Hydroxide Nanoparticles for Targeted Cellular Uptake Through Clathrin-Mediated Endocytosis

ARTICLE *in* CHEMISTRY - AN ASIAN JOURNAL · JANUARY 2009

Impact Factor: 4.59 · DOI: 10.1002/asia.200800290 · Source: PubMed

CITATIONS

80

READS

74

5 AUTHORS, INCLUDING:



Jae-Min Oh

Yonsei University

78 PUBLICATIONS 2,325 CITATIONS

SEE PROFILE



Soo-Jin Choi

Seoul Women's University

57 PUBLICATIONS 1,568 CITATIONS

SEE PROFILE



Jin-Ho Choy

Ewha Womans University

478 PUBLICATIONS 9,858 CITATIONS

SEE PROFILE

# Inorganic Metal Hydroxide Nanoparticles for Targeted Cellular Uptake Through Clathrin-Mediated Endocytosis

Jae-Min Oh,<sup>[a, b]</sup> Soo-Jin Choi,<sup>[a, c]</sup> Go-Eun Lee,<sup>[a]</sup> Jung-Eun Kim,<sup>[a]</sup> and Jin-Ho Choy<sup>\*[a]</sup>

**Abstract:** Layered double hydroxides (LDHs) are biocompatible materials which can be used as drug-delivery nanovehicles. In order to define the optimum size of LDH nanoparticles for efficient cellular uptake and drug-delivery pathway, we prepared different sized LDH nanoparticles with narrow size distribution by modulating the crystal growth rate, and labelled each LDH particle with a fluorophore using a silane coupling reaction. The cellular

uptake rate of LDHs was found to be highly dependent on particle size ( $50 > 200 \geq 100 > 350$  nm), whose range of 50 to 200 nm was selectively internalized into cells through clathrin-mediated endocytosis with enhanced permeability and retention. Our study clearly shows

**Keywords:** cell adhesion • cellular uptake • drug delivery • layered compounds • nanoparticles

that not only the particle size plays an important role in the endocytic pathway and processing, but also the size control of LDH nanoparticles results in their targeted uptake to site-specific clathrin-mediated endocytosis. This result provides a new perspective for the design of LDH nanoparticles with maximum ability towards targeted drug delivery.

## Introduction

Biocompatible nanoparticles, like inorganic layered double hydroxides (LDHs), possessing negligible toxicity, high anionic exchange capacity, and pH dependent solubility, have attracted increasing attention as nano-carriers for drugs and bio-active molecules.<sup>[1–4]</sup> Recently, a number of studies have focused on the interaction between nanoparticles and biological systems to understand their trafficking at the systemic and cellular level and to develop new strategies

for the design of efficient drug-delivery nano-carriers.<sup>[5–12]</sup> As is well documented, macromolecules or nanoparticles could be transported into cells through a process called endocytosis. In particular, pinocytosis occurs in all cell types and is mediated by at least four basic mechanisms: macropinocytosis, clathrin-mediated endocytosis, caveolae-mediated endocytosis, and clathrin-caveolae and dynamin-independent endocytosis.<sup>[13]</sup>


Many physical, chemical, and biological factors, such as particle size, surface characteristics, and physiological conditions, can influence both the cellular interactions and systemic distribution. Among various factors, particle size has been considered to play an important role in the adhesion to plasma membrane, cellular uptake, and subsequent intracellular processing, especially for nanoparticles less than 500 nm in size.<sup>[14]</sup> In order to induce an even bio-distribution and to prolong plasma half-life, it is generally understood that the drug-delivery nanovehicles should be small enough (less than 200 nm) to avoid non-selective uptake by macrophages of the reticuloendothelial system in the liver and spleen,<sup>[15]</sup> but larger than 5 nm (molecular weight 30000 to 40000) to escape by rapid renal clearance.<sup>[16]</sup> In fact, a few researches have emphasized the importance of the particle size on cellular uptake in DNA/cationic polymer nanocomposite or glycoviruses,<sup>[17,18]</sup> and suggest their upper size limit for efficient endocytic internalization. However, to the best of our knowledge, no information is currently available on

[a] Prof. Dr. J.-M. Oh,<sup>+</sup> Prof. Dr. S.-J. Choi,<sup>+</sup> G.-E. Lee, J.-E. Kim, Prof. Dr. J.-H. Choy  
Center for Intelligent Nano-Bio Materials  
Division of Nanosciences BK21  
Department of Chemistry and Nano Science  
Ewha Womans University, Seoul 120-750, Korea  
Fax: (+82)2 3277 4340  
E-mail: jhchoy@ewha.ac.kr

[b] Prof. Dr. J.-M. Oh<sup>+</sup>  
Department of Chemistry and Medical Chemistry  
College of Science and Technology, Yonsei University  
Wonju, Gangwondo 220-720, Korea

[c] Prof. Dr. S.-J. Choi<sup>+</sup>  
Department of Food Science and Technology  
Seoul Women's University, Seoul, 139-774, Korea

[<sup>+</sup>] Equal contribution to the work.

 Supporting information for this article is available on the WWW under <http://dx.doi.org/10.1002/asia.200800290>.

the particle-size effect of inorganic nanovehicles upon interaction with cells.

Until now, most of the studies have focused on the simple evaluation of drug efficacy or the cellular internalization rate of drug-LDH composites.<sup>[2–4,19–21]</sup> It is not easy to evaluate the relationship between the efficacy and particle size because of the broad size distribution of LDH nanoparticles (from several tens nanometers up to few micrometer, when prepared by conventional coprecipitation method) and the lack of luminescence from LDH itself, which makes cellular tracing difficult.

In this study, we have successfully prepared LDH nanoparticles with uniformly controlled sizes under hydrothermal conditions, with a fluorophore conjugated to the surface, by means of the crystal growth mechanism and inorganic-organic coupling reaction. Finally, with the well-defined LDH nanoparticles, the particle size effects on the entry, cellular uptake, and intracellular retention were systematically investigated to establish the relationship between LDH particle size and cellular uptake behavior.

## Results and Discussion

In order to verify the effect of size on the cellular uptake of LDH, we prepared different sized LDH particles with narrow size distribution, while maintaining the chemical properties such as structure, composition, and surface charge. In this study, four different particles (50, 100, 200, and 350 nm) with a narrow size distribution were synthesized by intentionally restricting the crystal growth rate and by applying hydrothermal conditions. The crystal growth of LDH particles is known to proceed in two steps, namely, nucleation (formation of seed) and crystal growth (aging). According to the crystal growth theory,<sup>[22]</sup> growth rate can be expressed as  $dL/dt = C \exp(-1/RT)$  (with particle size  $L$ , time  $t$ , nutrient concentration  $C$ , temperature  $T$ , gas constant  $R$ ), and thus the particle size of the product can be varied by adjusting the reaction temperature  $T$  and time  $t$ . Therefore, for the 50 nm sized particles, the reaction time for crystal growth after nucleation was minimized (~12 h), which resulted in small crystallites as shown in Figure 1A(a). To obtain particles with 100, 200, and 350 nm, the crystal

growth step was uniformly controlled under hydrothermal conditions in order to induce partial dissolution-precipitation at the surface of the nanoparticles, and thus give rise to a homogeneous particle size distribution. As expected from the above equation, the particle size becomes larger with an increase in reaction time and temperature (Figure 1A). All the LDH nanoparticles showed narrow size distribution as shown in Figure 1B. It is noteworthy that the cell parameters and chemical compositions of LDHs thus prepared were found to be the same (Table 1).

For effective tracing of the pathway through the cell membrane and quantitative evaluation of cellular uptake, different-sized LDHs were labeled with luminescent fluorescent 5'-isothiocyanate (FITC). The covalent bonding between FITC and LDH was realized with a silane coupling reaction and thiourea bond formation (Scheme 1). The surface hydroxyl groups of LDH were modified by (3-aminopropyl)triethoxysilane (APS), and then the amine terminal of APS and the isothiocyanate terminal of FITC were covalently conjugated to result in a thiourea bond. The grafting of APS and the subsequent conjugation of FITC molecules to LDH nanoparticles was verified by infrared spectroscopy. The FT-IR spectra (Figure 2) showed the sequential conjugation of APS and FITC. Upon APS grafting, the peak at  $450\text{ cm}^{-1}$ , attributed to M–O–M (M: metal such as Mg and Al) vibration in the brucite layer (asterisks in Figure 2C), became fairly broadened with a peak maximum at  $480\text{ cm}^{-1}$ , which mainly results from the superimposition of bands that correspond to Si–O–Al ( $530\text{ cm}^{-1}$ ) and Si–O–Mg ( $472\text{ cm}^{-1}$ ) in LDH-APS and LDH-FITC. The distinct peaks at  $1250$  and  $1160\text{ cm}^{-1}$  in LDH-APS (arrows in Figure 2B) could be attributed to (Si–CH<sub>2</sub>) and (Si–OEt), respectively, which confirms the presence of the silane group, and the small peak around  $1600$ – $1700\text{ cm}^{-1}$  (dotted circle in Figure 2B) results from the primary amine groups ( $\delta\text{-NH}_2$ ). In the spectrum of LDH-FITC, the peaks at  $1630$ ,  $1578$ , and  $1459\text{ cm}^{-1}$  (diamonds in Figure 2B) are characteristic of C=O, C–N–H, and N–H bonds, respectively, and the peak at  $1109\text{ cm}^{-1}$  (triangle) results from the C–O–C group in the FITC molecules. Furthermore, the peak at  $2040\text{ cm}^{-1}$ , which represents the thiocyanate group (rectangle in Figure 2B) of FITC, disappeared after conjugation to LDH because of the formation of a thiourea bond. Also, solid state <sup>29</sup>Si-NMR and UV/Vis spectroscopic results confirm the step-by-step conjugation of APS and FITC on the LDH surface (see Supporting Information). Thus, it is evident that there is sequential grafting of APS and FITC onto the LDH, and the FITC molecules are strongly bound to the LDH nanoparticles.

It is noteworthy that the physico-chemical properties of the LDHs, such as crystal structure, size, chemical compositions, and positive surface charge, remain unchanged even after conjugation (Figure 3, Table 1) although LDHs were fluorescently labeled by covalent conjugation of FITC molecules as verified by FT-IR. The powder X-ray diffraction patterns of LDH at each conjugation step revealed that the crystal structure of LDH was not influenced by the grafting

### Abstract in Korean:

금속 이중층 수산화물 (LDH) 은 생체친화성 층상 물질로서 나노 약물 전달체로 이용될 수 있다. 효율적인 세포 내 유입 경로를 위한 LDH 나노입자의 최적 크기를 구하기 위하여 결정 성장 속도를 적절히 조절하여 균일한 분포를 갖는 다양한 크기의 나노입자를 제조하였고, 실란 결합 반응을 통하여 입자를 형광으로 표지하였다. LDH 나노입자의 세포 내 유입 속도는 입자 크기에 영향을 많이 받는 것으로 나타났고 ( $50 > 200 \geq 100 > 350\text{ nm}$ ), 특히  $50 - 200\text{ nm}$  의 크기를 갖는 입자는 클라트린을 매개로 하는 엔도시토시스를 선택하여 때문에 세포 침투율이 높으며, 세포 내 유지 효율도 향상되는 것으로 관찰되었다. 본 실험 결과에 따라 나노입자의 크기가 세포 내 유입 경로를 선택하는 데 중요한 역할을 한다고 밝혀졌으며, LDH 나노입자는 크기를 조절함에 따라 특정한 엔도시토시스 경로를 선택한다는 것을 알 수 있었다. 이러한 연구 결과는 표적지향성 및 약물 전달 효율이 극대화된 LDH 나노입자를 디자인 하는 데 새로운 전망을 제시할 것이다.

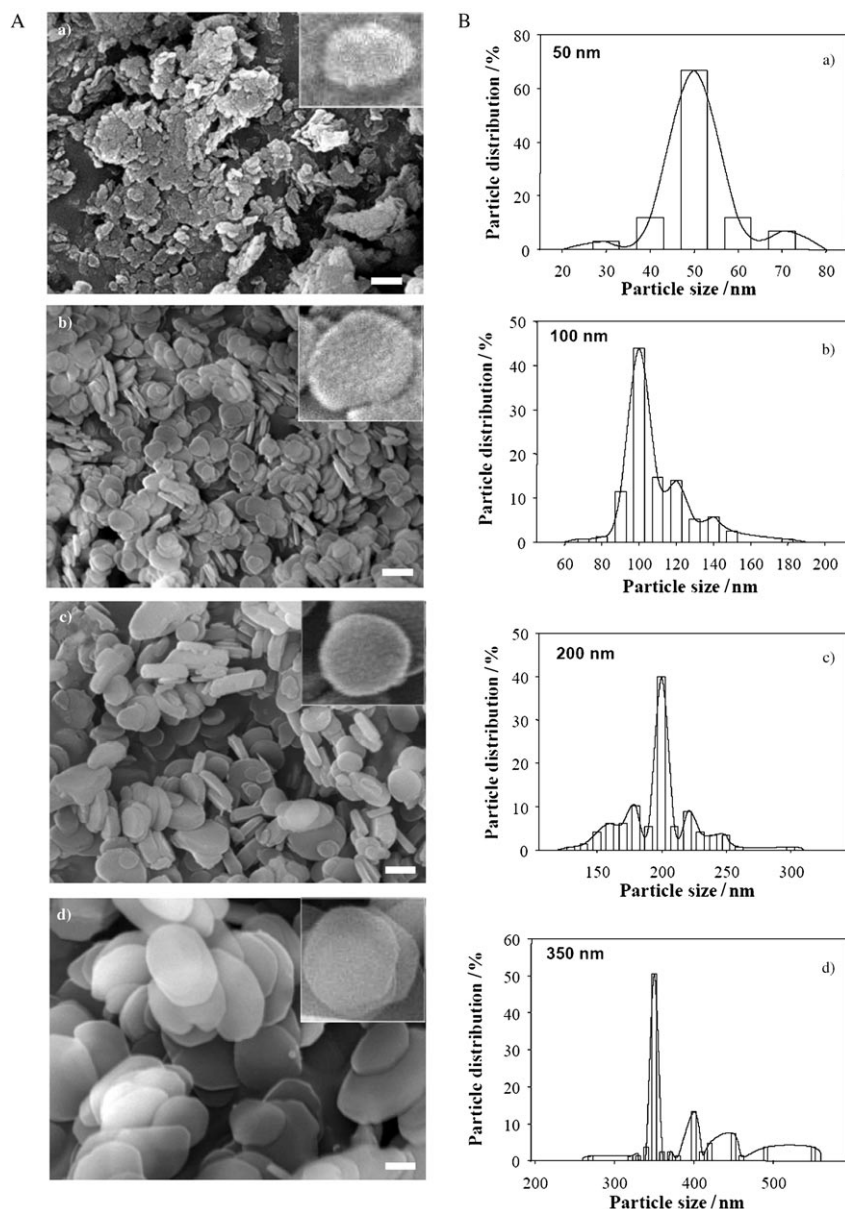


Figure 1. Field emission scanning electron microscope (FE-SEM) images (A) and the corresponding histogram of particle size distribution (B) for LDHs with 50 nm (a), 100 nm (b), 200 nm (c), and 350 nm (d). For the histogram, 200 grains were randomly selected from SEM images of each sample and the sizes were measured particle by particle. The inset images in (A) are the magnification of one particle, and the scale bar in (A) stands for 100 nm.

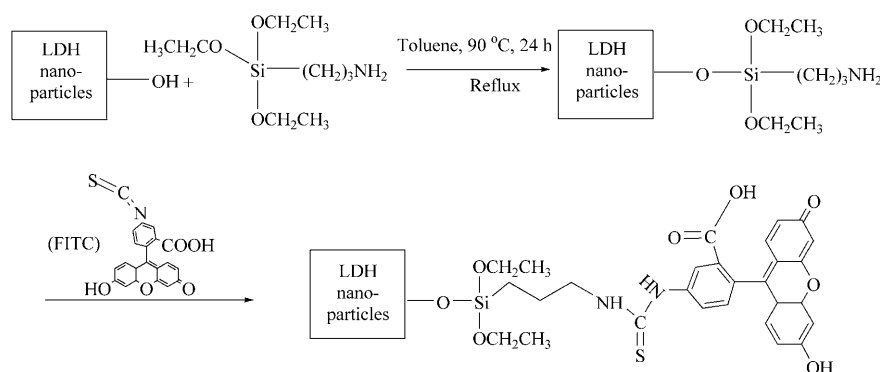
reaction. The metal atoms on the surface do not have a saturated coordination sphere, and thus produce more reactive sites at the radial edge than in the bulk material. Therefore, the grafting reaction was expected to preferentially occur in the edge region as illustrated in Figure 3. Quantitative analysis results (chemical composition in Table 1 and Table S1 in the Supporting Information) also confirmed that only a part of the LDH surface was modified. Surprisingly, this partial modification did not change the properties of the LDH nanoparticles.

In the present study, we have focused on the size-dependent internalization pathways of the nanoparticles. Human osteosarcoma (MNNG/HOS) cells were incubated with different-sized LDH-FITC molecules for 2 h and their accumulations in the cells were analyzed by flow cytometry. As shown in Figure 4A, the cells took up considerable amounts of LDH particles up to a size of 200 nm, but very little uptake of the 350 nm particles was observed. This is an indication that cellular uptake is highly related to particle size ( $50\text{ nm} > 200\text{ nm} > 100\text{ nm} > 350\text{ nm}$ ). A large uptake of 50 nm LDH particles might be because of their high positive surface charge<sup>[23]</sup> compared to the larger particles (Table 1), which gives rise to an enhanced interaction between LDH and the negatively charged cell membrane. On the other hand, the 100 nm and 200 nm particles showed similar cellular uptake behavior compared to those with a size of 50 and 350 nm (Figure 4A), although the cellular uptake of the 200 nm particles was higher and the presence of serum did not affect the cellular uptake of LDHs (Figure 4B). It is, therefore, concluded that internalization of LDHs is not mediated by their non-specific adsorption on serum proteins, but mediated by their own entry pathways.

As shown in Figure 5A, the cellular uptake of LDHs as a function of incubation time strongly depends on the particle size. The internalization of 100 and 200 nm particles were found to be quite similar and reached a plateau after 2 h. The 50 nm LDHs, however, were rapidly internalized, which shows a maximum at the very early stage of incubation time, but no significant increase could be seen for the 350 nm LDH. All the nanoparticles with the four different sizes were internalized into the cells in a concentration dependent manner, and reached a plateau at 200 to  $500\text{ }\mu\text{g mL}^{-1}$  depending on the particle size (Figure 5B). In addition, we have also studied the particle retention inside the cells (Figure 5C). The cells were treated with LDHs,

Table 1. Particle sizes, cell parameters, zeta potentials and chemical formulae for different sized LDHs before and after grafting FITC (\*Zeta potentials were measured with respect to pH values, and the data shown stands for the zeta potential at neutral pH (~7)). Cell parameters stand for the unit cell parameters of hexagonal LDH nanoparticles.

Sample	Before grafting FITC (pristine LDH)				After grafting FITC (LDH-FITC)			
	Particle size [nm]	Cell parameters [Å]	Zeta potential* [mV]	Chemical formula	Particle size [nm]	Cell parameters [Å]	Zeta potential* [mV]	Chemical formula
50 nm LDH	51 (±8)	$a=3.04$ $c=22.7$	+30	$\text{Mg}_{0.68}\text{Al}_{0.32}(\text{OH})_2 \cdot (\text{CO}_3)_{0.16} \cdot 0.1 \text{H}_2\text{O}$	50 (±7)	$a=3.04$ $c=22.7$	+30	$\text{Mg}_{0.68}\text{Al}_{0.32}(\text{OH})_2 \cdot (\text{CO}_3)_{0.16} \cdot 0.1 \text{H}_2\text{O}$ -APS <sub>0.032</sub> -FITC <sub>0.002</sub>
100 nm LDH	108 (±16)	$a=3.04$ $c=22.7$	+27	$\text{Mg}_{0.68}\text{Al}_{0.32}(\text{OH})_2 \cdot (\text{CO}_3)_{0.16} \cdot 0.1 \text{H}_2\text{O}$	109 (±15)	$a=3.04$ $c=22.7$	+13	$\text{Mg}_{0.68}\text{Al}_{0.32}(\text{OH})_2 \cdot (\text{CO}_3)_{0.16} \cdot 0.1 \text{H}_2\text{O}$ -APS <sub>0.013</sub> -FITC <sub>0.002</sub>
200 nm LDH	198 (±26)	$a=3.04$ $c=22.7$	+27	$\text{Mg}_{0.68}\text{Al}_{0.32}(\text{OH})_2 \cdot (\text{CO}_3)_{0.16} \cdot 0.1 \text{H}_2\text{O}$	200 (±28)	$a=3.04$ $c=22.7$	+5	$\text{Mg}_{0.68}\text{Al}_{0.32}(\text{OH})_2 \cdot (\text{CO}_3)_{0.16} \cdot 0.1 \text{H}_2\text{O}$ -APS <sub>0.006</sub> -FITC <sub>0.002</sub>
350 nm LDH	381 (±53)	$a=3.04$ $c=22.8$	+18	$\text{Mg}_{0.68}\text{Al}_{0.32}(\text{OH})_2 \cdot (\text{CO}_3)_{0.16} \cdot 0.1 \text{H}_2\text{O}$	375 (±50)	$a=3.04$ $c=22.8$	+2	$\text{Mg}_{0.68}\text{Al}_{0.32}(\text{OH})_2 \cdot (\text{CO}_3)_{0.16} \cdot 0.1 \text{H}_2\text{O}$ -APS <sub>0.003</sub> -FITC <sub>0.001</sub>



Scheme 1. Reaction scheme of APS grafting and subsequent FITC conjugation on LDH surface.

washed with PBS, and further incubated in fresh medium in the absence of LDHs. The 100, 200, and 350 nm LDHs were well retained in the cells during the entire incubation time, whereas the intracellular concentration of 50 nm LDH had decreased dramatically within the first 8 h, which suggests their possible efflux into the extracellular environment. It is likely that LDHs smaller than 100 nm behave differently compared to the larger particles because of their high surface areas and positive surface charge, which leads to easy endocytosis. The 50 nm LDH with a large surface area may decompose more rapidly than larger particles under acidic intracellular condition, and thus result in easy exocytosis.

To compare the localization of LDH-FITC with that of clathrin heavy chain (CHC) or caveolin-1 molecules, the cells were incubated with LDH-FITC, and then stained with either anti-CHC antibody or anti-caveolin-1 antibody both conjugated to Texas Red (TR). In order to study the possible unspecific uptake of the particles through macropinocytosis, the cells were pre-incubated with neutral dextran (70 kDa) conjugated to TR, a well-known marker of macropinocytosis, followed by incubation with LDH-FITC as described above. According to confocal microscopy studies, we found that each LDH-FITC, with sizes of 50, 100, and

200 nm, were highly colocalized with CHC, but not with caveolin-1 or neutral dextran (Figures 6 A, B, C). In contrast, 350 nm-sized LDH-FITC was colocalized with neither CHC nor caveolin-1.

To further confirm the size-dependent endocytosis of LDHs, we also investigated the uptake modulation after the inhibition of different endocytic pathways as follows. The cells were pre-incubated with endocytosis inhibitors (Supporting

Information) and then treated with LDH-FITC for 2 h. The quantitative analysis of the cellular internalization of LDH-FITC was carried out by flow cytometry (Figure 7). The LDH uptake with each size (50, 100, and 200 nm) was found to be considerably suppressed after inhibiting the clathrin-mediated endocytosis (chlorpromazine (cpz) or potassium depletion; 80–85 % lower depending on the particle size), which indicates that clathrin proteins play an important role in the internalization of LDHs. The cellular uptake of the 350 nm-sized particles was not significantly affected by the inhibition, which indicates that the large particles might not be selective in endocytic pathways. It is, therefore, concluded that LDHs with a size range of 50 to 200 nm can be primarily internalized into cells through clathrin-mediated endocytosis and this is highly correlated with efficient cellular uptake as shown in Figure 4.

## Conclusions

As clearly demonstrated, the clathrin-mediated endocytosis is mainly responsible for the efficient internalization of LDH nanoparticles with an upper limit of 200 nm in size.



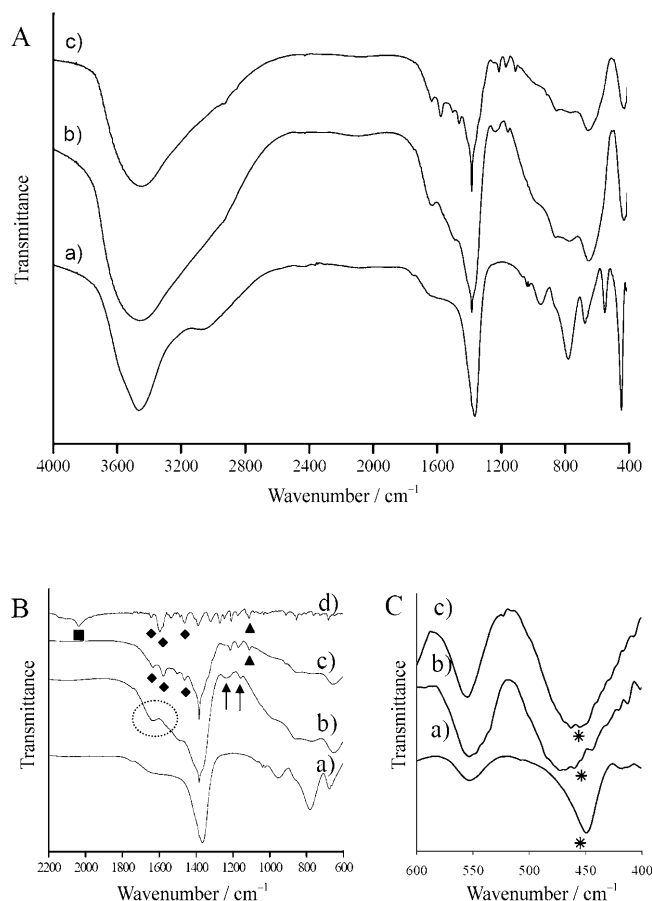


Figure 2. Fourier transform infrared (FT-IR) spectra for a) pristine LDH, b) APS grafted LDH, c) APS-FITC grafted LDH, and d) FITC. B and C are magnified spectra in the region of 1800–600 and 600–400  $\text{cm}^{-1}$ , respectively. ( $\uparrow$ : Si–C stretching of APS,  $\blacktriangle$ : C–O–C stretching of FITC,  $\blacklozenge$ : C=O, N–H, C–N–H stretching of FITC  $\blacksquare$ : thiocyanate (SCN) stretching of FITC).

This is consistent with the low uptake of 350 nm LDH that results from a non-selective internalization pathway. In other words, our results show that targeted delivery of LDH nanoparticles through clathrin-mediated endocytosis can be achieved by controlling the particle size in the range of 50 to 200 nm. It is noteworthy that clathrin-mediated endocytosis is the most common uptake mechanism in all mammalian cells<sup>[13]</sup> and that the targeted delivery of drugs through site-specific clathrin-mediated endocytosis have recently attracted increasing interest for efficient uptake.<sup>[19,20]</sup> Therefore, particle size itself is indeed one of the important factors for cellular membrane surface to recognize alien nanoparticles and eventually the cellular internalization pathways. The present results on size optimization for efficient targeted cellular uptake

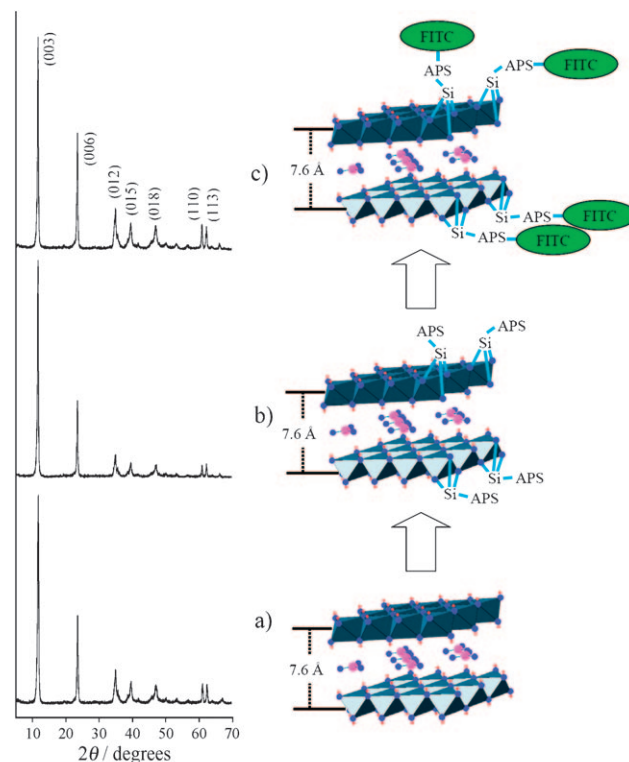


Figure 3. Powder X-ray diffraction patterns and corresponding schematic structures of LDHs at each reaction step a) pristine LDH, b) APS grafted LDH, and c) FITC grafted LDH.

provide a new perspective to design LDH nanovehicles with maximized ability towards drug delivery.

## Experimental Section

### Preparation of LDHs with Different Particle Sizes and their FITC-Grafted Forms

LDH with the formula of  $\text{Mg}_{0.68}\text{Al}_{0.32}(\text{OH})_2(\text{CO}_3)_{0.16} \cdot 0.1\text{H}_2\text{O}$  was prepared by the coprecipitation method. A solution containing  $\text{Mg}(\text{NO}_3)_2 \cdot 6\text{H}_2\text{O}$  (0.088 M) and  $\text{Al}(\text{NO}_3)_3 \cdot 9\text{H}_2\text{O}$  (0.044 M) was titrated with a solution of  $\text{NaOH}/\text{NaHCO}_3$  (0.5 M/0.5 M) until the pH reached  $9.5 \pm 0.1$ . For 50 nm LDH particles, the titrated solution was vigorously stirred at 25 °C for 12 h. Whereas LDHs with larger particle sizes (100, 200, and 350 nm) could be obtained when the aqueous solutions were hydrothermally

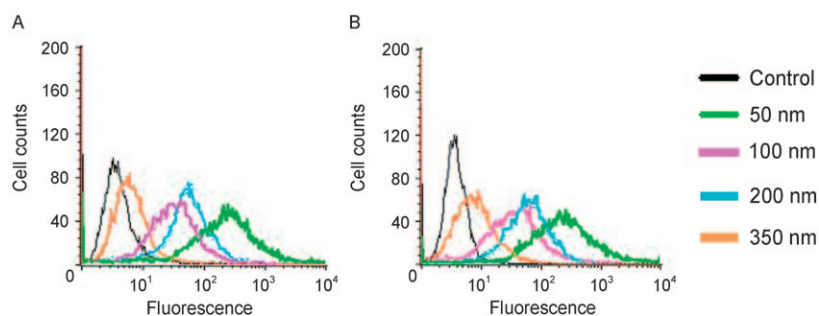


Figure 4. Intracellular uptake of LDH-FITC as a function of LDH size in the absence (A) and presence (B) of serum in MNG/HOS cells.

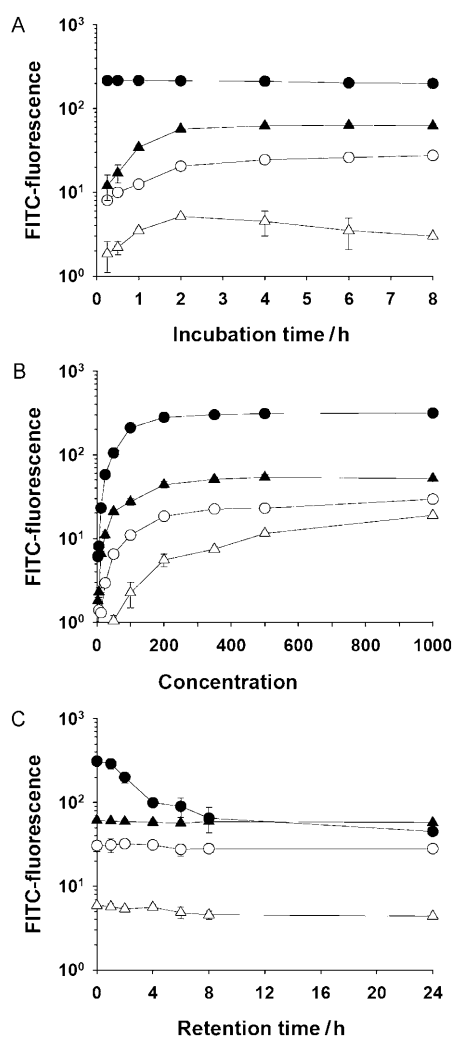


Figure 5. Cellular uptake and retention kinetics of four different-sized LDHs: cellular uptake of LDHs as a function of incubation time (A), concentration-dependent cellular uptake of LDHs (B), and retention of LDHs in the cells (C). ● 50 nm, ○ 100 nm, ▲ 200 nm, △ 350 nm.

treated after titration. The synthetic conditions for 100, 200, and 350 nm particles were 100°C for 12 h, 200°C for 24 h, and 200°C for 48 h, respectively. The white precipitate obtained was collected by centrifugation, washed several times with de-ionized water, and then freeze-dried.

The surfaces of the pristine LDHs with different particle sizes were first modified by grafting the amino silane<sup>[26]</sup> whose amine end was then conjugated with fluorescein 5'-isothiocyanate (FITC). Each LDH (1 g) was put in a flask and heated at 100°C for 12 h under vacuum in order to achieve anhydrous reaction conditions. After dehydration, N<sub>2</sub> was filled in the flask and anhydrous toluene containing 0.5 mL of (3-aminopropyl)-triethoxysilane (APS) was added to the LDH powder and stirred for 24 h at 60°C. The obtained slurry was isolated, washed with toluene to remove unreacted APS, and then freeze-dried. The thus prepared white powder was dispersed in deionized water, and FITC/EtOH solution was then added and the mixture was stirred vigorously at 37°C for 12 h to induce a thiourea bond between the amine group of APS and the thiocyanate group of FITC. The LDHs thus modified were separated by centrifugation, washed with water/EtOH, and then freeze-dried.

#### Characterization of LDH Nanoparticles

Each LDH sample was characterized by powder X-ray diffraction (Rigaku X-ray diffractometer with the monochromated beam of Cu-K<sub>α</sub>

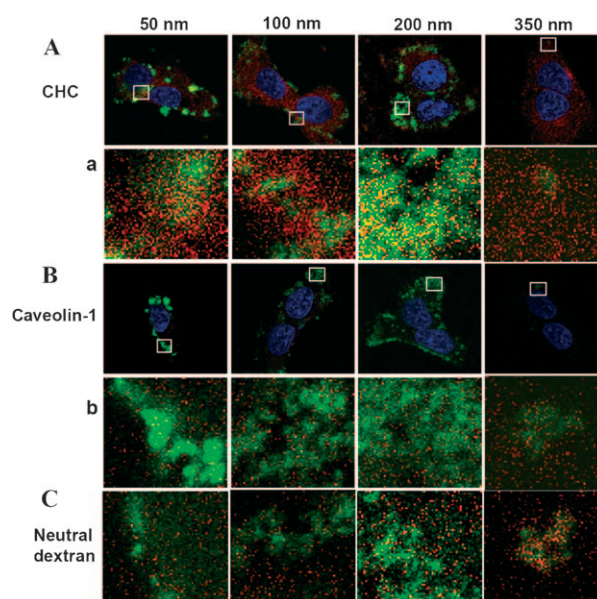


Figure 6. Size effect of LDHs on the endocytic pathway. Confocal microscopic images of LDH-FITC-treated MNNG/HOS cells, showing high colocalization of 50, 100, and 200 nm LDHs with CHC (A), but not with caveolin-1 (B) or neutral dextran (C). a, b; magnified images of the boxes in (A) and (B). Green, blue, and red colors represent LDH-FITC, DAPI-stained nuclei, and TR-conjugated CHC, caveolin-1 or neutral dextran, respectively.

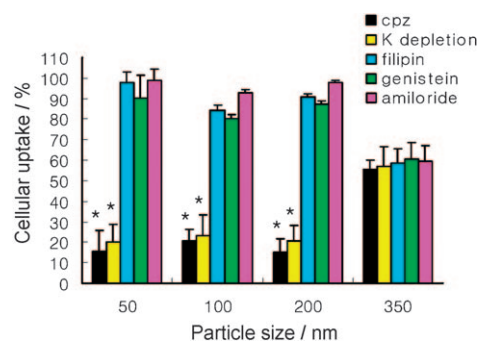


Figure 7. Effects of endocytic inhibitors on the internalization of LDH-FITC. Cellular uptake (%) of LDHs was calculated by comparison with that in the absence of inhibitor (100%) for each particle size. \* Significant difference from control ( $p < 0.05$ ).

radiation ( $\lambda = 1.5418 \text{ \AA}$ ) and infrared spectroscopy (FT-IR, JASCO FT/IR-6100) analyses using the standard KBr disk method. The particle size and surface charge (zeta potential) of LDHs were determined by scanning electron microscopy (SEM; JEOL JSM-6700F) and a zeta potentiometer (Malvern Instrument Zeta Potentiometer 3000), respectively. For the chemical composition of the LDH, elemental analysis (CHNS, LECO Corp (Michigan, USA)), inductive coupled plasma-atomic emission analysis (ICP, Shimadzu (Columbia, USA)), and thermogravimetry (TG, pyris diamond TG-DTA, Perkin-Elmer, at a heating rate of  $5^\circ\text{Cmin}^{-1}$  under an ambient atmosphere) experiments were carried out. All the stoichiometric measurements were carried out in triplicate. The significant number in chemical formulae (Table 1) was only considered to two decimal places for pristine LDHs, and three decimal places for APS and FITC grafted LDHs. The coefficients of FITC in Table 1 have an error range of  $0.002 \pm 0.03$  (for 50, 100, and 200 nm LDH) and  $0.001 \pm 0.0001$  (for 350 nm LDH).

### Cell Culture

Human osteosarcoma (MNNG/HOS) cells were purchased from ATCC (American Type Culture Collection). The cells were grown in MEM medium (Welgene, Ltd) supplemented with 10% heat inactivated fetal bovine serum, 100 units mL<sup>-1</sup> penicillin, and 100 µg mL<sup>-1</sup> streptomycin in a humidified atmosphere (5% CO<sub>2</sub> plus 95% air) at 37°C.

### Fluorescence-Activated Cell Sorter (FACS) Analysis of Cellular Uptake and Intracellular Retention

The cells were treated with a given concentration of LDH-FITC, and the accumulation of LDH-FITC in the cells was analyzed by using a FACS Calibur (Becton Dickinson BD). The cells incubated in the absence of the nanoparticles were used as control. The cells (2.5 × 10<sup>5</sup> mL<sup>-1</sup>) were incubated overnight at 37°C under a 5% CO<sub>2</sub> atmosphere and the cellular uptake of LDHs was measured by incubating the cells with 100 µg mL<sup>-1</sup> LDHs in MEM medium in the presence or absence of serum for the given incubation times. The cellular retention of LDHs was studied by pre-incubating the cells with 200 µg mL<sup>-1</sup> LDHs for 2 h, washing with PBS, and further incubating in fresh medium without LDHs. Endocytic pathway inhibitors, 10 µg mL<sup>-1</sup> chlorpromazine (CPZ), potassium-free buffer (140 mM NaCl, 20 mM Hepes, 1 mM CaCl<sub>2</sub>, 1 mM MgCl<sub>2</sub>, 1 mg mL<sup>-1</sup> D-glucose, pH 7.4), 1 µg mL<sup>-1</sup> filipin, 200 µM genistein, and 100 µM amiloride hydrochloride, were also used to examine cellular uptake modulation, by pre-incubating the cells with the endocytic inhibitor for 1 h at 37°C, followed by incubation with 100 µg mL<sup>-1</sup> LDH-FITC for 2 h. The cells were washed twice with PBS, harvested by scraping, and then suspended in PBS containing 0.1% BSA. The data shown is the mean fluorescence obtained from a population of 10000 cells. The cells incubated in the absence of particles were used as control (CTRL). The experiment was repeated at least three times on separate days. Statistical analyses for all the data were performed on the basis of Student's *t* test and *P* values < 0.05 were considered as significant ones.

### Immunofluorescence/Confocal Microscopy

MNNG/HOS cells were seeded on 12-well slides (5 × 10<sup>3</sup> cells/well) and incubated with 100 µg mL<sup>-1</sup> LDH-FITC for 2 h. The cells were washed with ice-cold PBS several times, fixed with freshly made 3% formaldehyde (containing 1.5% methanol) in PBS (pH 7.4) for 15 min, and permeabilized with 0.1% Triton X-100 in PBS for 10 min. The cells were incubated with primary antibodies against mouse clathrin heavy chain (CHC) and caveolin-1 (BD Biosciences) for 1 h, washed and then incubated with secondary antibodies conjugated to TR (Molecular Probes). Vesicles undergoing macropinocytosis were labeled by pre-incubation with 5 µM TR-labeled neutral dextran (70 kDa, Molecular Probes) for 20 min followed by incubation with LDH-FITC as described above. The cells were then stained with 2 µg mL<sup>-1</sup> DAPI dye for 10 min at room temperature in the dark. The cells were washed and visualized using a Zeiss LSM 510 confocal microscope (Carl Zeiss Inc., Germany) equipped with an Argon (488 nm) and HeNe (543 nm) laser for fluorescence studies. Image acquisition and analysis were carried out with LSM 510 software. Each experiment was repeated three times on separate days.

### Statistical Analysis

Statistical analyses were performed using Student's *t* test for unpaired data, and *P* values < 0.01 were considered significant. Data are presented as means ± SEM.

## Acknowledgements

We thank Dong-Ok Kim for her help in supporting cell preparations. This work was supported by the Korea Science and Engineering Foundation (KOSEF) grant funded by the Korea government (MEST) (No. R11-2005-008-00000-0) and partly by MKE (Ministry of Knowledge Economy) through the National R & D project for Nano Science and Technology (grant: 2005-0980-1 and 2005-0546-1).

- [1] L. Desigaux, M. B. Belkacem, P. Richard, J. Cellier, P. Leone, L. Cario, F. Leroux, C. Taviot-Gueho, B. Pitard, *Nano Lett.* **2006**, *6*, 199–204.
- [2] J. H. Choy, S. Y. Kwak, Y. J. Jeong, J. S. Park, *Angew. Chem.* **2000**, *112*, 4207–4211; *Angew. Chem. Int. Ed.* **2000**, *39*, 4041–4045.
- [3] J. H. Choy, J. S. Jung, J. M. Oh, M. Park, J. Jeong, Y. K. Kang, O. J. Han, *Biomaterials* **2004**, *25*, 3059–3064.
- [4] J. H. Choy, S. Y. Kwak, J. S. Park, Y. J. Jeong, J. Portier, *J. Am. Chem. Soc.* **1999**, *121*, 1399–1400.
- [5] N. W. S. Kam, H. J. Dai, *J. Am. Chem. Soc.* **2005**, *127*, 6021–6026.
- [6] C. C. Berry, *J. Mater. Chem.* **2005**, *15*, 543–547.
- [7] N. W. Kam, Z. Liu, H. Dai, *Angew. Chem.* **2006**, *118*, 591–595; *Angew. Chem. Int. Ed.* **2006**, *45*, 577–581.
- [8] D. M. Huang, Y. Hung, B. S. Ko, S. C. Hsu, W. H. Chen, C. L. Chien, C. P. Tsai, C. T. Kuo, J. C. Kang, C. S. Yang, C. Y. Mou, Y. C. Chen, *FASEB J.* **2005**, *19*, 2014–2016.
- [9] I. I. Slowing, B. G. Trewyn, V. S. Y. Lin, *J. Am. Chem. Soc.* **2006**, *128*, 14792–14793.
- [10] S. Giri, B. G. Trewyn, M. P. Stellmaker, V. S. Y. Lin, *Angew. Chem.* **2005**, *117*, 5166–5172; *Angew. Chem. Int. Ed.* **2005**, *44*, 5038–5044.
- [11] F. Torney, B. G. Trewyn, V. S. Y. Lin, K. Wang, *Nature Nanotech.* **2007**, *2*, 295–300.
- [12] Y. S. Lin, C. P. Tsai, H. Y. Huan, C. T. Kuo, Y. Hung, D. M. Huang, Y. C. Chen, C. Y. Mou, *Chem. Mater.* **2005**, *17*, 4570–4573.
- [13] S. D. Conner and S. L. Schmid, *Nature* **2003**, *422*, 37–44.
- [14] K. Y. Win, S. S. Feng, *Biomaterials* **2005**, *26*, 2713–2722.
- [15] S. M. Moghimi, A. C. Hunter, J. C. Murray, *Pharmacol. Rev.* **2001**, *53*, 283–318.
- [16] J. Fang, T. Sawa, T. Akaike, T. Akuta, S. K. Sahoo, G. Khaled, A. Hamada, H. Maeda, *Cancer Res.* **2003**, *63*, 3567–3574.
- [17] C. Jong-Yuh, W. Petra van, T. Herre, J. A. C. Daan, E. H. Wim, *Pharm. Res.* **1996**, *13*, 1038–1042.
- [18] T. Nakai, T. Kanamori, S. Sando, Y. Aoyama, *J. Am. Chem. Soc.* **2003**, *125*, 8465–8475.
- [19] J. H. Choy, S. Y. Kwak, J. S. Park, Y. J. Jeong, *J. Mater. Chem.* **2001**, *11*, 1671–1674.
- [20] J. M. Oh, S. J. Choi, S. T. Kim, J. H. Choy, *Bioconjugate Chem.* **2006**, *17*, 1411–1417.
- [21] J.-M. Oh, M. Park, S.-T. Kim, J.-Y. Jung, Y.-G. Kang, J.-H. Choy, *J. Phys. Chem. Solids* **2006**, *67*, 1024–1027.
- [22] J. Nyvlt, *The Kinetics of Industrial Crystallization*, Vol. 19, Elsevier, Amsterdam, **1985**.
- [23] D. W. Lim, Y. I. Yeom, T. G. Park, *Bioconjugate Chem.* **2000**, *11*, 688–695.
- [24] H. Li, Z. M. Qian, *Med. Res. Rev.* **2002**, *22*, 225–250.
- [25] A. Widera, F. Norouziyan, W. C. Shen, *Adv. Drug Delivery Rev.* **2003**, *55*, 1439–1466.
- [26] A. Y. Park, H. Kwon, A. J. Woo and S. J. Kim, *Adv. Mater.* **2005**, *17*, 106–109.

Received: July 25, 2008

Published online: November 5, 2008